Phonon linewidth in III-V semiconductors from density-functional perturbation theory

Alberto Debernardi
Max-Planck-Institut für Festkörperforschung, Heisenbergstrasse 1, 70569 Stuttgart, Germany
(Received 19 December 1997)

In this work we present an *ab initio* calculation of the Raman linewidth of transverse and longitudinal phonon in zinc-blende semiconductors GaAs, AlAs, GaP, and InP. We propose a simple approximation that permits us to calculate the longitudinal linewidths with the same computational effort as the transverse ones. The microscopic mechanisms responsible for the decay are analyzed and discussed. The temperature dependence of the linewidths is computed. Our results are in good agreement with available experimental data up to room temperature for both transverse and longitudinal optical modes and give reliable predictions in materials difficult to study experimentally. [S0163-1829(98)00420-2]

I. INTRODUCTION

One of the most spectacular achievements of solid state physics in this century is the microscopic understanding of the vibrational properties of crystals. The phonon spectra of different materials have been extensively investigated in recent decades[1] both theoretically and experimentally.

In a perfect harmonic crystal, phonons do not interact with each other, so that a nonequilibrium phonon population would persist in time.[2] However, one experimentally observes that the phonon population decays towards equilibrium on a time scale of a few picoseconds. The anharmonic decay of phonons into vibrations of lower frequency is a fundamental mechanism for energy relaxation in semiconductors, as it controls the formation and time evolution of the nonequilibrium phonon populations that are emitted by high-density excited carriers when they decay towards their ground state.[3]

Experimentally, anharmonic lifetimes of individual zone-center phonons can be extracted from their measured Raman linewidths if inhomogeneous broadening effects can be neglected. Menéndez and Cardona have obtained the full temperature dependence for elemental semiconductors more than a decade ago.[4] This task, however, is much more difficult in systems, such as heterostructures, where composition and/or strain inhomogeneities add to the usual (e.g., isotopic[5]) elastic broadening factors. Experiments in the time domain by ultrafast spectroscopies have also become available in recent years and provide useful information, especially for long lifetime phonons. In fact, such phonons display extremely narrow Raman linewidths, and to obtain the measure of the phonon lifetime with Raman spectroscopy one must deconvolute the measured Raman line to take into account the contribution to the Raman linewidth due to the spectrometer resolution, which, in this case, has approximately the same size as the contribution to the linewidth due to anharmonic decay.

II. THEORY OF PHONON LIFETIME

In the following we summarize the procedure that has to be implemented to compute the phonon lifetime and introduce the notation used throughout this work. The detailed theory of anharmonic broadening of Raman lines can be found in several review articles (see, for example, Refs. 4, 6, and references therein).

We indicate the ionic positions at equilibrium as

$$\mathbf{R}_s^l = \mathbf{R}^l + \tau_s ,$$

where l is a cell index and s $(s=1,...,n)$ is a basis index in the unit cell of n atoms. We introduce the displacements $\{\mathbf{u}_s^l\}$ of the ions from their equilibrium positions; Greek subscripts will be used to indicate Cartesian components.

The Taylor expansion of the total energy around the equilibrium positions in terms of the displacements reads

$$E_{\rm tot}(\{\mathbf{u}_s^l\}) = E_{\rm tot}^{(0)} + E_{\rm tot}^{(2)}(\{\mathbf{u}_s^l\}) + E_{\rm tot}^{(3)}(\{\mathbf{u}_s^l\}) + \cdots . \quad (2.1)$$

The second order term is the harmonic contribution to the total energy, from which one can obtain the dynamical matrix and compute the phonon frequencies.

The third order term of a Taylor expansion of the total energy around the equilibrium positions in terms of the displacements reads

$$E_{\rm tot}^{(3)}(\{\mathbf{u}_s^l\}) = \frac{1}{6} \sum_{ll'l'',ss's'',\alpha\beta\gamma} \frac{\partial^3 E_{\rm tot}}{\partial u_{s,\alpha}^l \partial u_{s',\beta}^{l'} \partial u_{s'',\gamma}^{l''}} u_{s,\alpha}^l u_{s',\beta}^{l'} u_{s'',\gamma}^{l''} . \quad (2.2)$$

The displacements of the atoms from equilibrium are related to the phonon creation and annihilation operators, $a_j^+(\mathbf{q})$ and $a_j(\mathbf{q})$, through the usual second quantization formula,

$$u_{s,\alpha}^l = \sum_{\mathbf{q},j} \left(\frac{\hbar}{2\omega_j(\mathbf{q}) M_s N} \right)^{1/2} e_{s,\alpha}(\mathbf{q},j) e^{i\mathbf{q}\cdot\mathbf{R}^l} \times [a_j^+(-\mathbf{q}) + a_j(\mathbf{q})], \quad (2.3)$$

where M_s is the mass of the sth atom in the unit cell, N is the number of unit cells in the crystal, ω_j are the phonon frequencies, the j's label the phonon branches ($j=1-6$ in bulk compound semiconductors), and $e(\mathbf{q},j)$ is the amplitude of the jth phonon mode at wave vector $\mathbf{q}$ in the first Brillouin zone. Inserting Eq. (2.3) in Eq. (2.2), we obtain the third order correction to the total energy written in second quantization (terms of destruction and creation phonon operators).

The harmonic Hamiltonian does not induce transitions between states with different phonon populations. To study phonon decay times, we consider $E_{\rm tot}^{(3)}$ as a perturbation and use Fermi's golden rule. We thus obtain

$$\Gamma = \frac{2\pi}{\hbar}\sum_f |\langle i|E_{\rm tot}^{(3)}|f\rangle|^2 \delta(E_i - E_f), \tag{2.4}$$

where $|i\rangle$ and $|f\rangle$ label the initial and final states, respectively, E_i and E_f the corresponding energies, and the δ function ensures energy conservation. At thermal equilibrium the phonon population is described by the Bose-Einstein distribution

$$n_j(\mathbf{q}) = \frac{1}{e^{\hbar\omega_j(\mathbf{q})/kT}-1}.$$

It is easy to verify that the third order interaction produces no change in such a population, i.e., a thermal phonon population is stable, as it was obvious *a priori*. We assume that at $\mathbf{q}=\mathbf{0}$ there is a nonequilibrium phonon population, while in all the other q points of the Brillouin zone the phonon population is given by the thermal occupation numbers. This is the so-called single-mode relaxation time approximation.[7] In our case, only the terms proportional to $a_{\rm LTO}(0)a_{j_1}^+(-\mathbf{q})a_{j_2}^+(\mathbf{q})$ and $a_{\rm TO}(0)a_{j_1}(\mathbf{q})a_{j_2}^+(\mathbf{q})$ give a nonvanishing contribution (LTO labels the longitudinal or transverse optical modes).

If only three-phonon processes are considered, energy and crystal momentum conservation dictates that the zone-center LTO phonon decays into a pair of phonons with opposite wave vectors, $\pm\mathbf{q}$, whose frequencies sum up to the frequency of the decaying mode. This is the only mechanism one must consider for the decay of a LO phonon. When we consider the decay of a TO phonon at the Brillouin zone center, one has to take into account the decay process in which the TO phonon is destroyed together with a phonon at $\mathbf{q}$, to create another phonon with a frequency that is the sum of the frequencies of the destroyed phonons and wave vector $\mathbf{q}$.

The inverse lifetime of the LTO mode at zone center reads

$$\begin{aligned}\Gamma_{\rm LTO} = \frac{\pi}{2\hbar^2}\sum_{\mathbf{q},j_1,j_2}\left|V\begin{pmatrix}\mathbf{0} & \mathbf{q} & -\mathbf{q}\\ \rm LTO & j_1 & j_2\end{pmatrix}\right|^2 \{&[n_{j_1}(\mathbf{q}) + n_{j_2}(-\mathbf{q}) + 1]\delta[\omega_{\rm LTO}(\mathbf{0}) - \omega_{j_1}(\mathbf{q}) - \omega_{j_2}(-\mathbf{q})] \\ &+ 2[n_{j_1}(\mathbf{q}) - n_{j_2}(\mathbf{q})]\delta[\omega_{\rm LTO}(\mathbf{0}) + \omega_{j_1}(\mathbf{q}) - \omega_{j_2}(\mathbf{q})]\}.\end{aligned} \tag{2.5}$$

Since the LO is the higher phonon frequency in the material, the second term in curly brackets is nonvanishing only for the TO phonon. This term describe the phonon upconversion where the TO phonon is scattered by a thermal phonon [of frequency $\omega_{j_1}(\mathbf{q})$] into a phonon of higher frequency [$\omega_{j_2}(\mathbf{q})$]. The matrix elements that determine the width Γ are given by

$$\begin{aligned}V\begin{pmatrix}\mathbf{0} & \mathbf{q} & -\mathbf{q}\\ \rm LTO & j_1 & j_2\end{pmatrix} = \sum_{ss's'',\alpha\beta\gamma}&\left(\frac{\hbar^3}{8M_sM_{s'}M_{s''}\omega_{\rm LTO}(\mathbf{0})\omega_{j_1}(\mathbf{q})\omega_{j_2}(-\mathbf{q})}\right)^{1/2} \\ &\times\left(\frac{1}{\sqrt{n}}\sum_{l',l''}\frac{\partial^3 E_{\rm tot}}{\partial u_{s,\alpha}^{l}\partial u_{s',\beta}^{l'}\partial u_{s'',\gamma}^{l''}}e^{i\mathbf{q}\cdot(\mathbf{R}^{l'}-\mathbf{R}^{l''})}\right)e_{s,\alpha}(\mathbf{0},\rm LTO)e_{s',\beta}(\mathbf{q},j_1)e_{s'',\gamma}(-\mathbf{q},j_2).\end{aligned} \tag{2.6}$$

The ingredients of the above formula are the harmonic frequencies and displacements and the third order derivative of the total energy. All these ingredients can be computed, in a density-functional framework, using density-functional perturbation theory.

III. THIRD ORDER DERIVATIVE BY DENSITY-FUNCTIONAL PERTURBATION THEORY

The harmonic frequencies and atomic displacements corresponding to a phonon in semiconductors can be easily obtained using density-functional perturbation theory[8,9] by computing the linear response to a perturbation that, in our case, is a displacement of the atom from the equilibrium position. The linear response to a small perturbation is also sufficient to compute the third order derivative to the total energy with respect to the same perturbation. This is a particular case of the so-called ''$2n+1$'' theorem.[10] The formulation of this theorem in a density-functional framework is due to Gonze and Vigneron,[11] which gives an explicit formula for the third order derivative. This expression was subsequently reformulated by Debernardi and Baroni in an efficient way for numerical calculations.[12] This method was successfully applied to compute the anharmonic phonon coupling constant[12] and to study the phonon linewidth of elemental semiconductors[13,14] giving very good results compared to experimental data.[13,16]

It is convenient to switch to reciprocal space and to introduce the reciprocal-space anharmonic force constant defined as

$$\begin{aligned}&C_{ss's'',\alpha\beta\gamma}(\mathbf{q}_1,\mathbf{q}_2,\mathbf{q}_3) \\ &\quad= \frac{1}{\sqrt{N^3}}\sum_{l,l',l''}\frac{\partial^3 E_{\rm tot}}{\partial u_{s,\alpha}^{l}\partial u_{s',\beta}^{l'}\partial u_{s'',\gamma}^{l''}}e^{i\mathbf{q}_1\cdot\mathbf{R}^{l}}e^{i\mathbf{q}_2\cdot\mathbf{R}^{l'}}e^{i\mathbf{q}_3\cdot\mathbf{R}^{l''}},\end{aligned} \tag{3.1}$$

where the **q**'s are in the first Brillouin zone. We recall that the translational invariance of the system gives the condition

$$\mathbf{q}_1+\mathbf{q}_2+\mathbf{q}_3=\mathbf{G}, \tag{3.2}$$

where **G** is a reciprocal-lattice vector. We can easily recognize that $C_{ss's'',\alpha\beta\gamma}(\mathbf{0},\mathbf{q},-\mathbf{q})$ is the anharmonic term that appears in parentheses in the last line of Eq. (2.6). The atomic displacement in reciprocal space is defined as

$$\mathbf{u}_s(\mathbf{q})=\frac{1}{\sqrt{N}}\sum_l \mathbf{u}_s^l e^{-i\mathbf{q}\cdot\mathbf{R}^l}.$$

In the following we replace, for simplicity, the double index (s,α) by p $(p=1,...,3n)$. Using the formula for the derivative of many variable functions, we rewrite the anharmonic tensor in term of derivatives with respect to $\mathbf{u}(\mathbf{q})$:

$$C_{p,p',p''}(\mathbf{q}_1,\mathbf{q}_2,\mathbf{q}_3)=\frac{\partial^3 E_{\rm tot}}{\partial u_p(\mathbf{q}_1)\partial u_{p'}(\mathbf{q}_2)\partial u_{p''}(\mathbf{q}_3)}. \tag{3.3}$$

To calculate this term we evaluate the general expression for the third order derivatives with respect to a specific small parameter λ [Eqs. (9) and (10) of Ref. 12], which, in our case, will represent the phonon displacements $u_p(\mathbf{q})$.

From Eq. (9) of Ref. 12, the expression for the anharmonic force constants reads

$$\begin{aligned}C_{pp'p''}(\mathbf{q}_1,\mathbf{q}_2,\mathbf{q}_3)=&\tilde{E}_{pp'p''}(\mathbf{q}_1,\mathbf{q}_2,\mathbf{q}_3)+\tilde{E}_{p'pp''}(\mathbf{q}_2,\mathbf{q}_1,\mathbf{q}_3)\\&+\tilde{E}_{pp''p'}(\mathbf{q}_1,\mathbf{q}_3,\mathbf{q}_2)+\tilde{E}_{p''pp'}(\mathbf{q}_3,\mathbf{q}_1,\mathbf{q}_2)\\&+\tilde{E}_{p'p''p}(\mathbf{q}_2,\mathbf{q}_3,\mathbf{q}_1)\\&+\tilde{E}_{p''p'p}(\mathbf{q}_3,\mathbf{q}_2,\mathbf{q}_1).\end{aligned} \tag{3.4}$$

In our case, $\tilde{E}$ is the sum of an electronic part $\tilde{E}^{\rm el}$ plus an ionic contribution $\tilde{E}^{\rm ion}$, which is essentially the third derivative of an Ewald sum whose expression is given in Appendix A:

$$\tilde{E}_{pp'p''}(\mathbf{q}_1,\mathbf{q}_2,\mathbf{q}_3)=\tilde{E}^{\rm el}_{pp'p''}(\mathbf{q}_1,\mathbf{q}_2,\mathbf{q}_3)+\tilde{E}^{\rm ion}_{pp'p''}(\mathbf{q}_1,\mathbf{q}_2,\mathbf{q}_3).$$

With the help of Eq. (10) of Ref. 12, we find for the electronic contribution

$$\begin{aligned}\tilde{E}^{el}_{pp'p''}(\mathbf{q}_1,\mathbf{q}_2,\mathbf{q}_3)=&\sum_v \left\langle \frac{\partial\psi_v}{\partial u_p(\mathbf{q}_1)}\right| P_c \frac{\partial H}{\partial u_{p'}(\mathbf{q}_2)} P_c \left|\frac{\partial\psi_v}{\partial u_{p''}(\mathbf{q}_3)}\right\rangle - \sum_{vv'} \left\langle \frac{\partial\psi_v}{\partial u_p(\mathbf{q}_1)}\right| P_c \left|\frac{\partial\psi_{v'}}{\partial u_{p'}(\mathbf{q}_2)}\right\rangle \left\langle \psi_{v'}\right| \frac{\partial H}{\partial u_{p''}(\mathbf{q}_3)} \left|\psi_v\right\rangle\\&+\frac{1}{2}\int \frac{\partial^2 V_{\rm ion}(\mathbf{r})}{\partial u_{p'}(\mathbf{q}_2)\partial u_{p''}(\mathbf{q}_3)} \frac{\partial n(\mathbf{r})}{\partial u_p(\mathbf{q}_1)} d\mathbf{r}+\frac{1}{6}\int \frac{\partial^3 V_{\rm ion}(\mathbf{r})}{\partial u_p(\mathbf{q}_1)\partial u_{p'}(\mathbf{q}_2)\partial u_{p''}(\mathbf{q}_3)} n(\mathbf{r}) d\mathbf{r}\\&+\frac{1}{6}\int \frac{\delta^3 E_{xc}[n]}{\delta n(\mathbf{r})\delta n(\mathbf{r}')\delta n(\mathbf{r}'')} \frac{\partial n(\mathbf{r})}{\partial u_p(\mathbf{q}_1)} \frac{\partial n(\mathbf{r}')}{\partial u_{p'}(\mathbf{q}_2)} \frac{\partial n(\mathbf{r}'')}{\partial u_{p''}(\mathbf{q}_3)} d\mathbf{r}d\mathbf{r}'d\mathbf{r}'',\end{aligned} \tag{3.5}$$

where H and $|\psi_v\rangle$ are, respectively, the unperturbed self-consistent Hamiltonian and the corresponding wave functions, and $V_{\rm ion}(\mathbf{r})$ is the *bare* (pseudo)potential acting on the electrons:

$$V_{\rm ion}(\mathbf{r})=\sum_{\mathbf{R},s} v_s(\mathbf{r}-\mathbf{R}-\boldsymbol{\tau}_s),$$

v_s being the bare (pseudo)potential centered at the atomic site $\mathbf{R}+\tau$.

In this manner all ingredients necessary to compute the phonon coupling constants are obtained.

IV. RAMAN LINEWIDTHS FOR ZINC-BLENDE SEMICONDUCTORS

Compound semiconductors differ from the elemental ones in that they have two different atoms in the unit cell. The displacement of the atoms due to a longitudinal optical phonon in the long wavelength limit $(\mathbf{q}\to\mathbf{0})$ may induce an electric field with the same wave vector of the phonon; in semiconductors this electric field is not completely screened by electrons and adds to the restoring force acting on ions, thus modifying the phonon frequencies. This determines the splitting of transverse and longitudinal optical modes near the zone center,[17] as observed in the phonon spectra of polar semiconductors.[18]

The splitting of LO and TO frequencies can be predicted by the so called phenomenological theory due to Huang.[19] The presence of an electric field produced by the LO phonon determines a nonanalytic contribution to the dynamical matrix at the center of the Brillouin zone. This contribution was computed by Cochran and Cowley[20] for an ionic crystal of arbitrary symmetry and rederived by Pick, Cohen, and Martin,[21] using a microscopic formulation.

In zinc-blende semiconductors, the macroscopic electric field associated to the phonon displacement does not affect the frequencies of transverse phonons but only those of longitudinal ones; similarly, up to third order in **u** the calculation of transverse phonon lifetimes involves no nonanalytic contribution in the anharmonic dynamical tensor, while the calculation of the LO lifetimes requires including the effects of macroscopic electric field.

The difference in the electron density response between a longitudinal and an optical phonon in the long wavelength

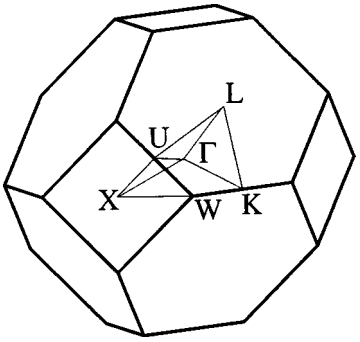

FIG. 1. Sketch of the Brillouin zone.

limit was discussed by Resta[22] for cubic materials with two atoms per unit cell. He showed that the first order correction to the density produced by a LO phonon can be written as

$$n_{\mathrm{LO}}^{(1)} = n_{\mathrm{TO}}^{(1)} - \frac{4\pi e Z^*}{\Omega \epsilon_\infty} n_E^{(1)}, \tag{4.1}$$

where $n_{\mathrm{TO}}^{(1)}$ is the change in the charge density induced by a TO mode, $n_E^{(1)}$ is the linear density response to a uniform electric field, Z^* the Born effective charges, e the electron charge, Ω the unit cell volume, and ϵ_∞ the high-frequency (electronic) dielectric tensor. The last term in the right-hand side of Eq. (4.1) represents the contribution due to the coupling of the LO phonon with the associated electric field and includes all nonanalytic terms. In this work the LO phonon lifetimes are computed neglecting the contribution due to $n_E^{(1)}$ (and the corresponding nonanalytical contribution to the wave-function response) in the anharmonic dynamical tensor. We will refer to this as the *zero field anharmonic approximation*, because in this approximation one sets the macroscopic electric field associated with the longitudinal phonon equal to zero; we propose this approximation as a suitable method to compute, without any further complication, the longitudinal linewidths in zinc-blende semiconductors.

V. COMPUTATIONAL INGREDIENTS

Compound semiconductors such as gallium arsenide and aluminum arsenide crystallize in the zinc-blende structure: the Bravais lattice is face-centered cubic with the two atoms per unit cell placed at $\tau_1 = 0$ and $\tau_2 = a/4(1,1,1)$, where a is the edge of the cube. The corresponding Brillouin zone is reported in Fig. 1. For a given configuration of the nuclei, we have assumed that the electrons are in the corresponding ground state (adiabatic approximation).

Calculations were performed within density-functional theory in the local-density approximation (LDA) for exchange and correlation energy. The input data for this approximation are the homogeneous electron gas exchange-correlation energy calculated with Monte Carlo techniques by Ceperley and Alder,[23] and interpolated by Perdew and Zunger.[24] We have used the same norm-conserving pseudopotentials as in Ref. 9, which were generated using a scheme proposed by von Barth and Car.[25] Our plane-wave basis sets are truncated to a kinetic-energy cutoff of 22 Ry for GaAs, AlAs, and GaP and to a cutoff of 20 Ry for InP, i.e., ~500 plane waves for all semiconductors we have investigated, which ensures a very accurate convergence in the third-order force constants. The Brillouin-zone integration over electronic states is performed using the special point technique.[26] We have used the (8,8,8) Monkhorst-Pack[27] integration mesh, which reduces to the 10-point Chadi-Cohen set[26] in the irreducible wedge. The reciprocal space integration over phonon states [the **q** points appearing in Eq. (2.5)] was performed using the tetrahedron method, introduced by Jepsen and Andersen[28] and independently by Lehmann and Taut.[29] With this method we have carried out the sum over the **q** points appearing in Eq. (2.5) using approximately 1500 points in the irreducible wedge of the Brillouin zone, so as to ensure a very accurate integration over the constant-energy surface given by the Dirac delta of Eq. (2.5). The integrand is calculated on a much coarser uniform mesh and then Fourier interpolated on the finer grid, much in the same way as phonon dispersions are obtained from selected calculations on a relatively coarse grid, passing through interatomic force constants.[9]

TABLE I. Equilibrium lattice parameter a (a.u.) obtained in the present calculation and the bulk modulus B_0 (Kbar). The parentheses contain the experimental values.

	a	B_0	ϵ_∞	Z^*
GaP	10.23	869	10.2	2.11
	(10.30)[a]	(1127)[a]	(9.08)[a]	(2.04)[b]
InP	10.94	757	10.4	2.45
	(11.09)[a]		(9.61)[a]	(2.55)[b]

[a]From Ref. 30.
[b]From Ref. 31.

To evaluate the expression for the phonon linewidth [Eqs. (2.5) and (2.6)] we need to compute the phonon frequencies and the corresponding eigenvectors. This was achieved using density-functional perturbation theory in the same way as Ref. 9; our phonon branches of GaAs and AlAs reproduce those presented in that work. We are not aware of first principles calculation of phonon dispersion in GaP and InP using density-functional perturbation theory. To show the reliability of our calculation in Tables I and II we report some of our results for lattice dynamical properties in GaP and InP compared with experimental data.

VI. COMPUTATIONAL RESULTS

In the following we present the results we have obtained for some III-V semiconductors. The LO and TO decay processes are *kinematically different*: as discussed previously in a polar semiconductor, the LO and TO branches are nondegenerate at **q** near zero, so energy conservation allows different decay processes with the creation of phonons in different regions of the Brillouin zone. As it was previously pointed out, the LO and TO decay processes are also *dynamically different*: due to the coupling with the electric field, an LO phonon induces a different density response than a transverse one. As a consequence, the dynamical tensors corresponding to LO and TO phonons are different.

Our results should therefore be considered exact within the LDA for TO phonons, while we have used the zero field

TABLE II. Phonon frequencies computed at high-symmetry points Γ, X, and L (in units of cm^{-1}). The parentheses contain experimental data (from Ref. 30).

	Γ_{LO}	Γ_{TO}	X_{TA}	X_{TO}	X_{LA}	X_{LO}	L_{TA}	L_{LA}	L_{TO}	L_{LO}
GaP	395	362	105	358	252	367	82	234	359	369
	(403)	(365)	(107)	(354)	(250)	(366)	(85)	(213)	(358)	(374)
InP	354	318	71	329	187	337	56	172	322	342
	(350)	(308)	(68)	(324)	(193)	(331)	(55)	(167)	(317)	(340)

anharmonic approximation for the anharmonic behavior of the LO phonons.

A. Lifetime of TO phonons

In Table III we report our results for the linewidths of transverse optical phonons at zero temperature. To the best of our knowledge, the only few experimental data are available in the literature at low temperature; for GaP they were obtained two decades ago by Bairamov, Kitaev, Negoduiko, and Khashkhozhev.[33] In a recent work, Irmer, Wenzel, and Monecke[34] measured the linewidth of GaAs and InP. The agreement between the experimental data and our results is good. In GaAs the discrepancy between our results and the experimental data of the TO linewidth can be attributed, at least in part, to the isotopic disorder of an experimental sample, which increased the Raman linewidth.[32]

To identify the relevant processes contributing to these results, in Table III we also report the relative weights of the individual decay channels, as obtained by restricting the sums over the j's in Eq. (2.5) to selected final states: ''TA'' ($j=1,2$), ''LA'' ($j=3$), and ''TO'' ($j=4,5$). The decay of a transverse phonon into one optical and one acoustic phonon is kinematically forbidden in all the present cases. It turns out that the dominant decay mechanisms are not the same in the four semiconductors. In GaAs and GaP, the process with maximum probability ($\simeq 96\%$) involves one LA and one TA mode as final states, and the *Klemens channel*, i.e., the decay of the LTO mode into two acoustic phonons belonging to the same branch and with opposite wave vectors, turns out to give a very small contribution. A similar situation was found for the decay of optical phonons at the Brillouin zone center for Si and Ge.[13] In AlAs and InP, instead, the Klemens channels LA+LA is the only kinematically allowed case by energy conservation.

TABLE III. Calculated full widths at half maximum ($2\Gamma_{TO}$) of zone-center transverse optical phonons at zero temperature. The corresponding experimental values are shown for comparison. The last columns indicate the relative contributions to the linewidth of the individual decay channels (see text).

	$2\Gamma_{TO}$ (cm^{-1})	$2\Gamma_{TO}$ (expt.) (cm^{-1})	LA+LA (%)	LA+TA (%)
GaAs	0.44	0.60[a]	4.5	95.5
GaP	2.97	3.06[b]	2.3	97.1
AlAs	0.13		100.0	
InP	0.49	0.50[a]	100.0	

[a]From Ref. 34.
[b]From Ref. 33.

In order to get a deeper insight into the microscopic mechanisms that determine the decay process, we plot in Fig. 2 the *wave-vector-resolved final state spectrum*, i.e., the **q**-dependent function that appears in Eq. (2.5) under the summation. Due to energy conservation, as expressed by the δ function, this quantity is nonzero only on a three-dimensional surface of which we display the intersection with some high-symmetry planes in the Brillouin zone (see also Fig. 1). The magnitude of the function on that surface (i.e., the magnitude of the matrix element responsible for the phonon decay) is represented by a rainbow color scale going from red to violet in order of increasing magnitude.

It is easy to identify the contribution of Klemens processes in the closed contour falling approximately midway between the Brillouin zone center and edge [this is where the LA phonon dispersion $\omega_{LA}(\mathbf{q})$ reaches the value $\omega_{LA}=\omega_{TO}/2$]. This is the only contribution allowed by energy conservation in AlAs and InP. In GaAs and GaP, the relevant contribution to the linewidth of TO phonons is due to the decay into a longitudinal and a transverse acoustic phonon. This contribution comes from wave vectors close to the Brillouin zone edge. In GaAs the latter decay mechanism is present in all the directions from Γ to the zone boundary. GaP shows a large value of the linewidth compared to the values obtained for the other materials. In particular, the main contribution corresponds to the decay of TO$\rightarrow$LA+TA phonons around the K point (see Fig. 2). The same decay mechanism is allowed by energy conservation also in the region around U and W points; in the other regions of the Brillouin zone the frequency of the TA branch is so low that no matching LA frequency exists yielding $\omega_{TA}(\mathbf{q})+\omega_{LA}(-\mathbf{q})=\omega_{TO}$.

B. Lifetime of LO phonons

Our results for LO phonons are shown in Table IV. In GaAs we compute $2\Gamma_{LO}=0.66\ cm^{-1}$; this value must be compared with the experimental one $\tau=9.2\pm0.6$ ps at 6 K, which corresponds to $2\Gamma_{LO}=0.58\ cm^{-1}$, as was obtained by Vallée and Bogani[35] using an infrared time-resolved coherent anti-Stokes Raman scattering (CARS). In the same material, Irmer *et al.*[34] measured $2\Gamma_{LO}=0.67\ cm^{-1}$, using Raman spectroscopy, while Kernohan *et al.*[36] obtained $2\Gamma_{LO}=0.35\ cm^{-1}$ with the same technique.

In GaP we have computed an LO-phonon linewidth $2\Gamma_{LO}=0.18\ cm^{-1}$. The lifetime was measured by Bron, Kuhl, and Rhee;[38,39] using CARS technique, they found $\tau=26.0\pm2.5$ ps (at 5 K), which corresponds to $2\Gamma_{LO}=0.20\pm0.02\ cm^{-1}$. They also measured the linewidth by spontaneous (incoherent) Raman scattering and found $2\Gamma_{LO}=0.23\ cm^{-1}$. A previous investigation performed by Baira-

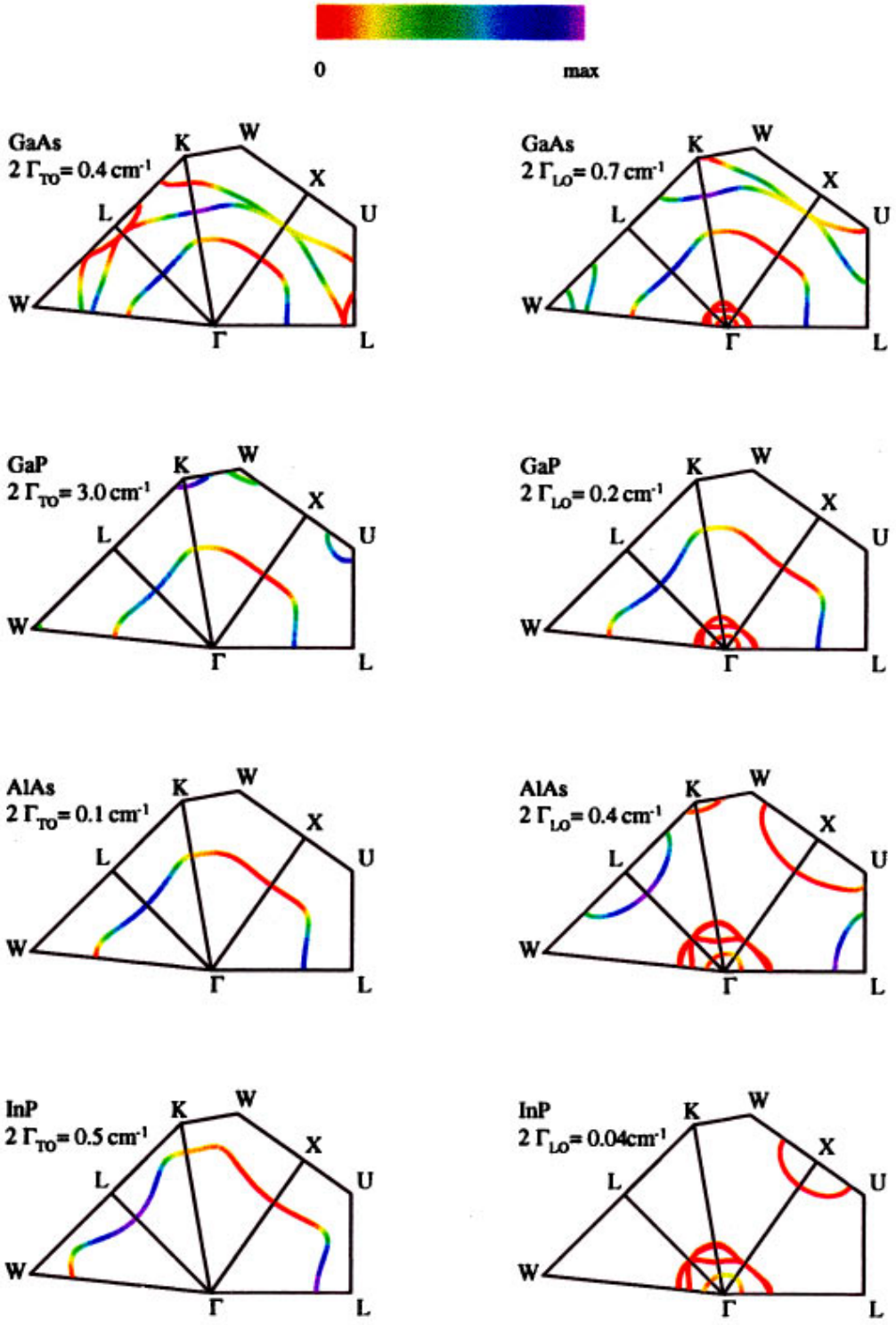

FIG. 2. (Color) Wave-vector-resolved final-state spectra of compound semiconductors at zero temperature. The color scale goes from red to violet in order of increasing magnitude. In each material, violet corresponds to the maximum contribution on the constant energy surface.

mov *et al.*[33] yielded $2\Gamma_{LO}=0.36\pm0.02$ cm^{-1} at 15 K.[41] In a subsequent work, Bairamov, Parshin, Toporov, and Ubaidullaev[40] measured $2\Gamma_{LO}=0.25$ cm^{-1}.

Our computation for the LO linewidths in InP gives $2\Gamma_{LO}=0.038$ cm^{-1}. Vallée measured the LO-phonon lifetime by CARS;[37] he obtained $2\Gamma_{LO}=0.026$ cm^{-1}. Using Raman spectroscopy, Irmer *et al.*[34] determined a phonon linewidth $2\Gamma_{LO}=0.15$ cm^{-1}. Kernohan *et al.*[36] measured $2\Gamma_{LO}=0.22$ cm^{-1}. This experimental value ''is consistent with recent results on time-resolved coherent anti-Stokes Raman scattering[37,42] when the effects of plasma-induced phonon dephasing are included.''[36] Our computed linewidth is in good agreement with the experimental value obtained by Vallée with time-resolved measurements; as discussed in the Introduction, we believe the technique used in this experiment is, in principle, more suitable than standard Raman

TABLE IV. Calculated full widths at half maximum ($2\Gamma_{LO}$) of zone-center longitudinal optical phonons at zero temperature and pressure. The corresponding experimental values are shown for comparison. The last columns indicate the relative contributions to the linewidth of the individual decay channels (see text).

	$2\Gamma_{LO}$ (cm^{-1})	$2\Gamma_{LO}$ (expt.) (cm^{-1})	LA+LA (%)	LA+TA (%)	TO+LTA (%)
GaAs	0.66	0.58±0.04[a]	4.0	96.0	
GaP	0.18	0.20±0.02[b]	96.0		4.0
AlAs	0.42		94.8		5.2
InP	0.038	0.026[c]	1.0		99.0

[a]From Ref. 35.
[b]From Ref. 39.
[c]From Ref. 37.

spectroscopy to determine the lifetime of phonons that display extremely narrow linewidths, such as the LO Raman line in InP. On the other hand, Raman spectroscopy will be more appropriate for measuring large linewidths (such as those displayed by GaAs at room temperature).

With the help of Table IV and Fig. 2, we can pinpoint the relevant LO decay processes. The decay of the LO phonon in GaAs shows mechanisms similar to those found in Si and Ge.[13] The most important decay mechanism involves two different branches: LA+TA. These processes correspond to the colored lines near the boundaries of the Brillouin zone in Fig. 2. In GaP and AlAs the relevant mechanism is the decay into the same longitudinal acoustic branch, as it is shown in the figure by the blue line around the L point.

The red lines around the Γ point refer to the decay channels LO→TO+LA and LO→TO+TA, which give a negligible contribution to the linewidth according to the fact that for this decay process the linewidths must vanish linearly with $|\mathbf{q}|$, when $\mathbf{q}$ approaches the Brillouin zone center (it is zero in GaAs where the allowed decay processes involve q points closer to the Γ point, a few percent in AlAs and GaP). We give the proof of this analytical behavior in Appendix B. The decay process of the LO phonon in InP is of particular interest. The linewidth is considerably smaller than those displayed by other material. We can easily understand the reason by looking at Fig. 2: the decay channel LO → LA + LA is allowed by energy conservation only in the region around the X point where the anharmonic matrix element which determine the width [given by Eq. (2.6)] gives only negligible contributions (red line in Fig. 2). The relevant decay mechanisms are LO→TO+LA and LO→TO+ TA (the red and yellow lines around the Brillouin zone center). In the long wavelength limit (i.e., when $\mathbf{q}$ goes to zero) this contribution to the linewidths must vanish. Since this is the only important decay process this explains why the LO-linewidth in InP is an order of magnitude smaller than in the other semiconductor considered in this work.

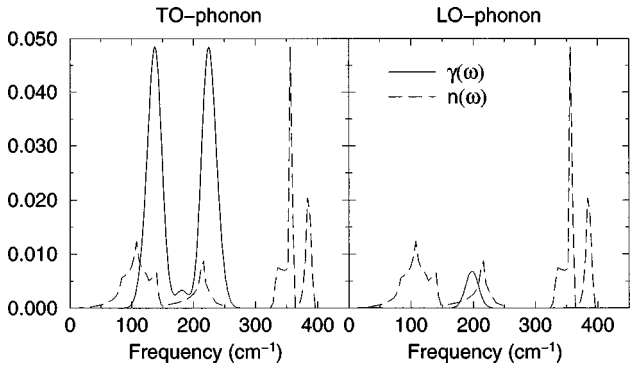

FIG. 4. Calculated phonon density of states, $n(\omega)$ (dashed line, arbitrary units), and frequency-resolved final state spectra, $\gamma(\omega)$ (solid line), at zero temperature in GaP. The vertical scale refers to $\gamma(\omega)$ (dimensionless).

C. Frequency resolved analysis

To improve further our analysis, we define the *frequency-resolved final state spectrum*, $\gamma(\omega)$, i.e., the probability per unit time that the LTO phonon decays into one mode of given frequency ω and one of frequency $\omega_{LTO}-\omega$. In practice, $\gamma(\omega)$ is obtained by restricting the sum over j_1 and $\mathbf{q}$ in Eq. (2.5) to those values for which $\omega_{j_1}(\mathbf{q})=\omega$ by inserting $\delta[\omega-\omega_{j_1}(\mathbf{q})]$ under the sign of sum. According to this definition, $\gamma(\omega)$ is symmetric around $\omega_{LTO}/2$ and the integral of $\gamma(\omega)$ over the whole range of frequencies is equal to $2\Gamma_{LTO}$. The *frequency-resolved final state spectra*, for TO and LO phonons in GaAs, GaP, AlAs, and InP, are displayed in Figs. 3, 4, 5, and 6, respectively.[48] The peak at $\omega_{LTO}/2$ corresponds to the Klemens decay mechanism. As anticipated in

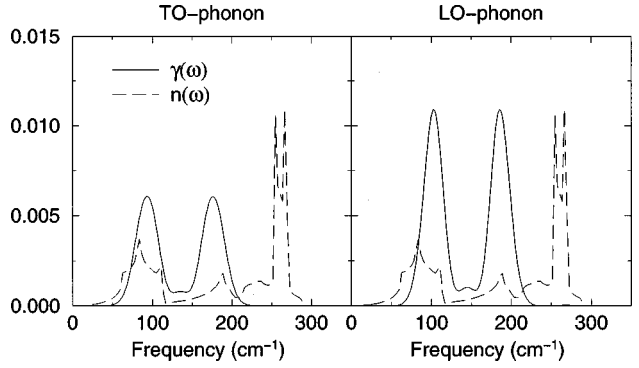

FIG. 3. Calculated phonon density of states, $n(\omega)$ (dashed line, arbitrary units), and frequency-resolved final state spectra, $\gamma(\omega)$ (solid line), at zero temperature in GaAs. Vertical scale refers to $\gamma(\omega)$ (dimensionless).

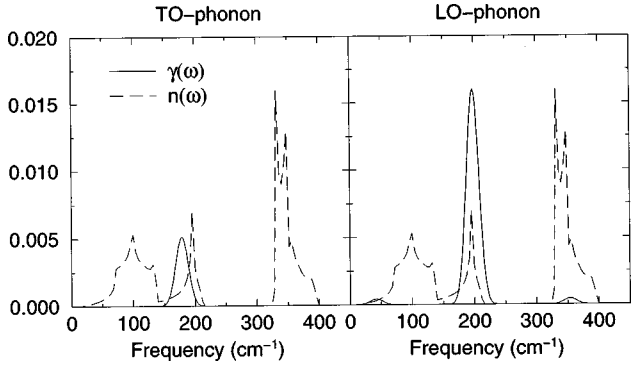

FIG. 5. Calculated phonon density of states, $n(\omega)$ (dashed line, arbitrary units), and frequency-resolved final state spectra, $\gamma(\omega)$ (solid line), at zero temperature in AlAs. The vertical scale refers to $\gamma(\omega)$ (dimensionless).

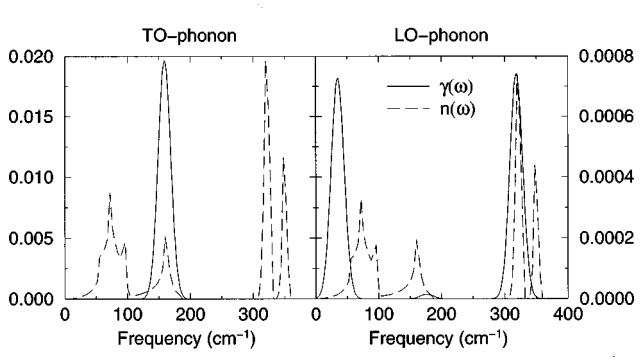

FIG. 6. Calculated phonon density of states, $n(\omega)$ (dashed line, arbitrary units), and frequency-resolved final state spectra, $\gamma(\omega)$ (solid line), at zero temperature in InP. The two vertical scales refer to $\gamma(\omega)$ (dimensionless).

the preceding sections, this peak is dominant in AlAs, while in GaAs the main contribution arises from the lateral peaks, symmetric with respect to $\omega_{\mathrm{LTO}}/2$. By comparison with the one-phonon density of state (DOS)—displayed in the figures as a dashed line—we notice that usually the main peak of $\gamma(\omega)$ is superimposed (or extremely close) to the Van Hove singularity of DOS, which corresponds to the longitudinal acoustic phonon at the zone border. For example, the LO phonon in AlAs or the TO phonon in InP presents a Klemens peak at the frequency of this Van Hove singularity, while in GaAs the same singularity in the DOS has the same frequency of one of the two lateral peaks. In the next section we will show how this kind of analysis can be useful to fit the temperature dependence of experimental linewidths.

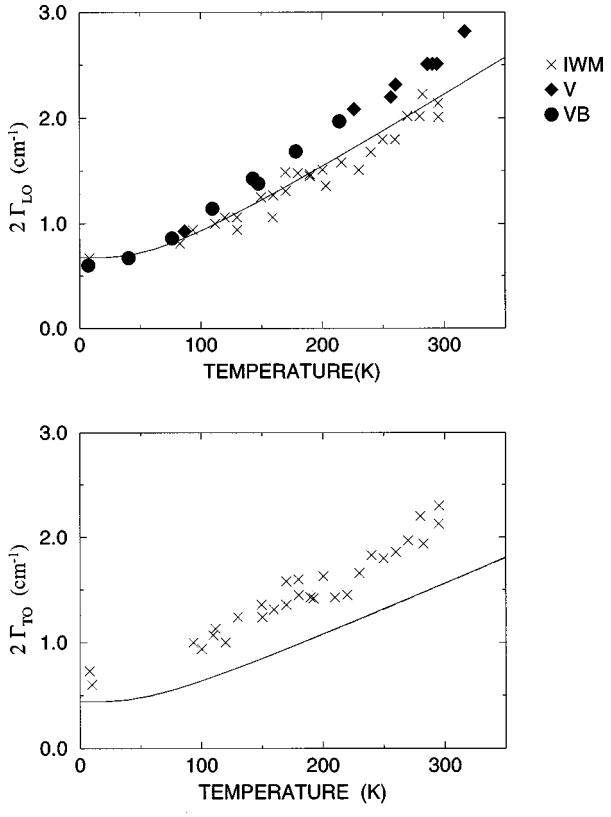

FIG. 7. Temperature dependence of the full width at half maximum, 2Γ, of the TO and LO phonons in GaAs. The solid lines represent the result of the present calculation; crosses denote experimental data from Ref. 34 (IWM); diamonds from Ref. 37 (V); and full circles from Ref. 35 (VB).

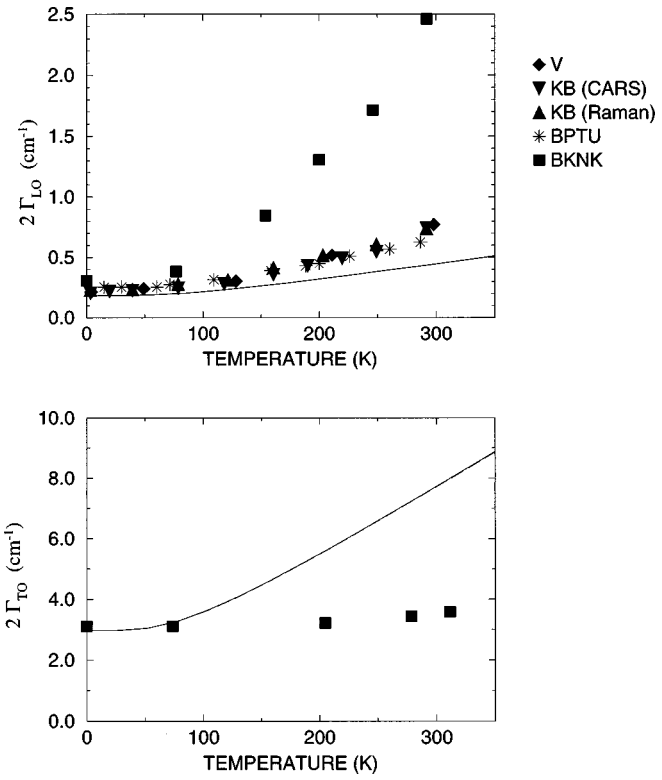

FIG. 8. Temperature dependence of the full width at half maximum, 2Γ, of the TO and LO phonons in GaP. The solid lines represent the result of the present calculation; diamonds denote experimental data from Ref. 37 (V); down and up triangles denote experimental data obtained by CARS and Raman width, respectively, from Ref. 38 (KB); stars represent experimental data from Ref. 40; squares represent experimental data from Ref. 33 (BKNK).

D. Temperature dependence

We have computed the temperature dependence of the linewidth for transverse and longitudinal optical phonons inserting the appropriate thermal occupation number in Eq. (2.5). Our results are shown in Figs. 7, 8, 9, and 10 for GaAs, GaP, AlAs, and InP, respectively; the continuous lines represent our theoretical results, the experimental data are denoted by symbols. As anticipated in Sec. II, the linewidth of the TO phonon is composed of two contributions given by the first and the second term of Eq. (2.5). The second term (corresponding to phonon up-conversion) vanishes at zero temperature, and, according to our calculation, is negligible in GaAs and GaP over the range of temperature we have considered, while it is small in AlAs and InP. The dashed line is the theoretical contribution arising from the first term in curly brackets of Eq. (2.5); with this scale the dashed line is superimposed on the continuous one in GaAs and GaP; the difference between the continuous and dashed lines is the phonon up-conversion contribution. By energy conservation the phonon up-conversion mechanism involves only phonons near the Brillouin zone center; from our analytic results of

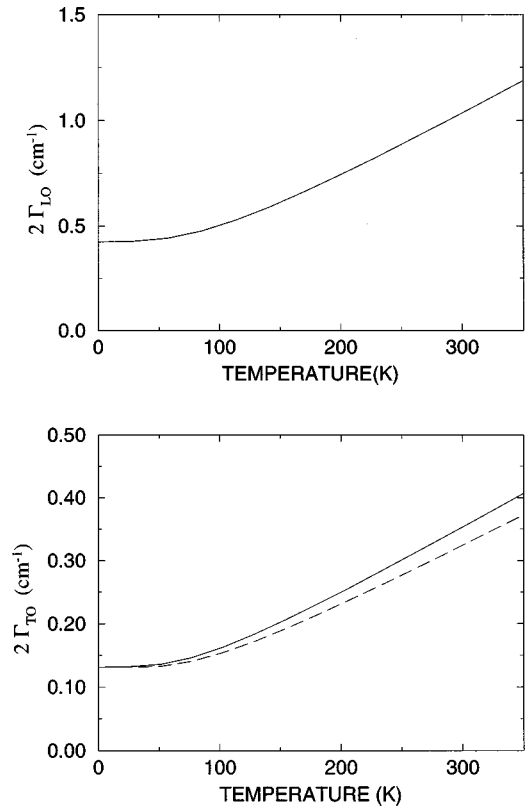

FIG. 9. Temperature dependence of the full width at half maximum, 2Γ, of the TO and LO phonons in AlAs. The solid lines represent the result of the present calculation; the difference between the solid and dashed lines denotes the contribution to the TO linewidth due to the phonon up-conversion (see text).

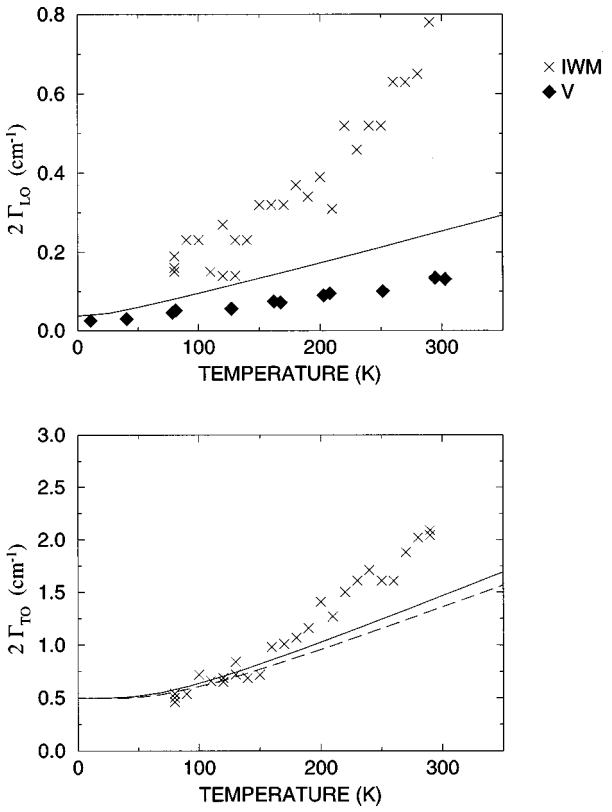

FIG. 10. Temperature dependence of the full width at half maximum, 2Γ, of the TO and LO phonons in InP. The solid lines represent the result of the present calculation; crosses denote experimental data from Ref. 34 (IWM); diamonds denote experimental data from Ref. 37 (V). The difference between the solid and dashed lines denotes the contribution to the TO linewidth due to the phonon up-conversion (see text).

Appendix B we can easily understand why the phonon up-conversion contribution is in general small compared to the other decay mechanisms.

The experimental data for $2\Gamma_{LO}$ in GaAs are due to Vallée and Bogani.[35] For completeness, we mention the earlier experimental data obtained by von der Linde *et al.*[43] at 77 K for the phonon lifetime of the LO Raman mode of GaAs. The same authors measured the time evolution of nonequilibrium incoherent optical phonons, finding $2\Gamma_{LO} = 0.76\ \text{cm}^{-1}$. At the same temperature they also measured the LO-phonon Raman linewidth $2\Gamma_{LO} = 0.85 \pm 0.1\ \text{cm}^{-1}$. At 77 K, Vallée *et al.* obtain $2\Gamma_{LO} = 0.83 \pm 0.05\ \text{cm}^{-1}$, in good agreement with our result of $2\Gamma_{LO} = 0.81\ \text{cm}^{-1}$.

In GaP our result for $2\Gamma_{TO}$ shows a strong temperature dependence. Our results are in good agreement with experimental data of Ref. 33 only at low temperature. In our opinion the discrepancies between theory and experiment may be explained, at least in part, by the observation that the relevant contribution in the computation of $2\Gamma_{TO}$ comes from decay processes in a small surface around the K point. The contribution to the linewidth due to this particular decay mechanism can be significantly modified, also at low temperature, by the high order contribution neglected in our computation. However, the Raman spectra measured at room temperature by Weinstein[44] and by Weinstein and Piermarini[45] displays a large TO linewidth in agreement with our result. We notice further that our results for the linewidth of the Raman modes of GaP at high temperature deviate from the experimental data of Ref. 33 for both TO and LO modes. The temperature dependence of $2\Gamma_{LO}$ in GaP is reported in Fig. 8. Our calculation agrees well with the experimental data of Bron, Kuhl, and Rhee[38] up to room temperature when the higher order corrections are expected to become important. The same agreement is found with the experimental data of Vallée[37] and with those of Bairamov, Parshin, Toporov, and Ubaidullaev.[40]

In Fig. 10 we show the temperature dependence of 2Γ in InP. Our computed $2\Gamma_{TO}$ is in good agreement with the experimental data of Irmer *et al.*[34] The temperature dependence of $2\Gamma_{LO}$ was measured by Vallée[37] using CARS and by Irmer *et al.* using conventional Raman spectroscopy.[34] Our computational results reproduce well Vallée's data, however because of the discrepancies between the two sets of experimental data, we believe that more experimental data are required in order to ascertain whether the discrepancy between theory and experiment is real, before embarking on an analysis to find its microscopic origin.

Finally, we mention how the frequency resolved analysis we have performed in Sec. VI C can be useful also in the analysis of experimental data. Up to room temperature, the temperature dependence of 2Γ is mainly determined by the zero temperature value of the linewidth multiplied by the appropriate thermal occupation number shown in Eq. (2.5). Using the frequency that corresponds to the main peak of the *frequency-resolved final state spectrum*, $\gamma(\omega)$ one can obtain

the linewidth at zero temperature by fitting the experimental data over a broad temperature range.

VII. CONCLUSIONS

In this work we have computed the phonon linewidths of the zone center optical phonon in compound semiconductors. Our results are in good agreement with available experimental data and give reliable predictions where the data are lacking. The zero field anharmonic approximation is shown to be a suitable method to compute the linewidths of longitudinal phonons. The mechanisms responsible for various decay processes are identified and discussed. In particular, we are able to explain why InP presents a LO linewidth that is an order of magnitude smaller than those of the other materials we have considered.

ACKNOWLEDGMENTS

The author is indebted to S. Baroni and M. Cardona for their interest in this work, many stimulating discussions and a critical reading of the manuscript. Thanks are also due to M. Wenzel for providing a tabulation of the experimental linewidth of Ref. 34, and to R. Resta, S. De Gironcoli, and E. Molinari for stimulating discussions.

APPENDIX A: IONIC TERM

The ionic term in the anharmonic force constants arises from the ion-ion Ewald contribution:[46]

$$E_{\mathrm{Ewald}}=\frac{4\pi N}{\Omega}\frac{e^2}{2}\left[\sum_{(\mathbf{G}\neq 0)}\frac{e^{-G^2/4\eta}}{G^2}\left|\sum_l Z_l e^{i\mathbf{G}\cdot\boldsymbol{\tau}_l}\right|^2-\frac{1}{4\eta}\left(\sum_l Z_l\right)^2\right]+\frac{Ne^2}{2}\sum_{l,m}\sum_R\frac{Z_l Z_m}{|\boldsymbol{\tau}_l-\boldsymbol{\tau}_m-\mathbf{R}|}\times[1-\mathrm{erf}(\sqrt{\eta}|\boldsymbol{\tau}_l-\boldsymbol{\tau}_m-\mathbf{R}|)]-Ne^2\left[\frac{\eta}{\pi}\right]^{1/2}\sum_l Z_l^2,$$

where Z_i indicates the bare ionic (pseudo)charge for the ith atom, Ω is the volume of the unit cell, and η is an arbitrary parameter, which may be chosen so large as to allow us to neglect the real-space term. After some straightforward algebra we find for the ionic contribution to the third order anharmonic constant

$$\begin{aligned}\tilde{E}^{\mathrm{ion}}_{ss's'',\alpha\beta\gamma}(\mathbf{q}_1,\mathbf{q}_2,\mathbf{q}_3)=&-\frac{2\pi e^2 N}{3\Omega}\sum_{(\mathbf{G}\neq 0)}\frac{e^{-G^2/4\eta}}{G^2}G_\alpha G_\beta G_\gamma Z_s\left[\sum_{\tilde{s}} Z_{\tilde{s}}\sin\mathbf{G}\cdot(\tau_{\tilde{s}}-\tau_s)\right]\delta_{s,s'}\delta_{s',s''}\\&+\frac{2\pi e^2}{\Omega}\sum_{(\mathbf{G}\neq 0)}\frac{e^{-(\mathbf{q}_2+\mathbf{q}_3+\mathbf{G})^2/4\eta}}{G^2}(q_{2,\alpha}+q_{3,\alpha}+G_\alpha)(q_{2,\beta}+q_{3,\beta}+G_\beta)(q_{2,\gamma}+q_{3,\gamma}+G_\gamma)\\&\times Z_s Z_{s'}\sin\mathbf{G}\cdot(\tau_s-\tau_{s'})\delta_{s',s''}.\end{aligned}\tag{A1}$$

APPENDIX B: ANALYTIC LIMIT

In this appendix we compute and discuss the analytical behavior of the contribution to the phonon lifetime due to decay processes that involve long-wavelength phonons. We define the quantity

$$2\Gamma_{j_1\to j_2+j_3}=\frac{\pi}{\hbar^2}\left|V\begin{pmatrix}\mathbf{q}&\mathbf{q}'&\mathbf{q}''\\ j_1&j_2&j_3\end{pmatrix}\right|^2.\tag{B1}$$

In Eq. (2.6) we have reported the expression of V in the case of decay of an optical phonon at Brillouin zone center (for the general expression, see Ref. 6). When we multiply $2\Gamma_{j_1\to j_2+j_3}$ by the thermal occupation number and integrate on the region of the Brillouin zone where the energy conservation is fulfilled, we obtain the contribution to the linewidth due to decay channel j_2+j_3. Our purpose is to study the behavior of $2\Gamma_{j_1\to+j_2+j_3}$ in the long-wavelength limit. In order to simplify the notation, we define the real space anharmonic force constants, which are the third derivatives of the total energy

$$C_{ss's'',\alpha\beta\gamma}(l,l',l'')=\frac{\partial^3 E_{\mathrm{tot}}}{\partial u^{l}_{s,\alpha}\partial u^{l'}_{s',\beta}\partial u^{l''}_{s'',\gamma}}.\tag{B2}$$

It is easy to prove that as a consequence of the translational invariance of the system, the anharmonic force constant must satisfy[15]

$$\sum_{l'',s''}C_{ss's'',\alpha\beta\gamma}(l,l',l'')=0.\tag{B3}$$

Let us consider a solid with a frozen-in phonon of small wave vector $\mathbf{q}$, defined by the ionic displacements in Eq. (2.3). We perform the usual decomposition,[47]

$$\frac{e_{s,\alpha}(\mathbf{q})}{\sqrt{M_s}}=u_{s,\alpha}(\mathbf{q})=u_\alpha(\mathbf{q})+\delta_{s,\alpha}(\mathbf{q}),$$

where the first term in the right-hand side is the displacement of the cell as a whole and the second the relative displacement of the two sublattices. They are called acoustic and optic components, respectively. In the limit of small $\mathbf{q}$, $u_\alpha(\mathbf{q})$ vanishes for optical modes while $\delta_{s,\alpha}(\mathbf{q})$ vanishes for acoustic modes. Expanding the phonon displacement with respect to the wave vector up to first order in $\mathbf{q}$, we find for the acoustic component

$$u_\alpha(\mathbf{q})=u_\alpha+\sum_\beta u_{\alpha,\beta}q_\beta,\tag{B4}$$

while the optical component becomes

$$\delta_{s,\alpha}(\mathbf{q})=\delta^s_\alpha+\sum_\beta \delta^s_{\alpha,\beta}q_\beta, \tag{B5}$$

with the condition

$$\sum_s M_s\delta^s_\alpha=0. \tag{B6}$$

From Eqs. (2.6) and (B2) we have that the contribution to the linewidth of a phonon in the j_ith branch ($2\Gamma_{j_1\to j_2+j_3}$) is proportional to the squared modulus of

$$\sum_{ss's'',\alpha\beta\gamma,l',l''} C_{ss's'',\alpha\beta\gamma}(l,l',l'')u_{s,\alpha}(\mathbf{q},j_1)u_{s',\beta}(\mathbf{q}',j_2)u_{s'',\gamma}(\mathbf{q}'',j_3)e^{-i(\mathbf{q}\cdot\mathbf{R}^l+\mathbf{q}'\cdot\mathbf{R}^{l'}+\mathbf{q}''\cdot\mathbf{R}^{l''})}. \tag{B7}$$

From the conservation of crystal momentum we have $\mathbf{q}+\mathbf{q}'+\mathbf{q}''=\mathbf{G}$, where $\mathbf{G}$ is a reciprocal-lattice vector. We now consider the displacements corresponding to an acoustic phonon $\mathbf{u}(\mathbf{q}',j_2)$ in the long-wavelength limit:

$$u_{s,\alpha}(\mathbf{q}',j_2)=u_\alpha(j_2)+\sum_\beta u^s_{\alpha,\beta}(j_2)q'_\beta, \tag{B8}$$

where the dependence on atomic position s is only in the term linear in $\mathbf{q}'$ (which includes a possible linear contribution of the optical component). Consider the contribution to the linewidth due to a decay process, which involves only one acoustic phonon ($2\Gamma_{\mathrm{O}\to A+\mathrm{O}}$) in the long-wavelength limit. Inserting the expansion (B8) in Eq. (B7) and expanding the exponential in powers of $\mathbf{q}'$ up to the first order, we obtain

$$\begin{aligned}&\sum_{ss's'',\alpha\beta\gamma,l',l''} C_{ss's'',\alpha\beta\gamma}(l,l',l'')u_{s,\alpha}(\mathbf{q},j_1)u_{s',\beta}(\mathbf{q}',j_2)u_{s'',\gamma}(\mathbf{q}'',j_3)e^{-i(\mathbf{q}\cdot\mathbf{R}^l+\mathbf{q}'\cdot\mathbf{R}^{l'}+\mathbf{q}''\cdot\mathbf{R}^{l''})}\\ &=\sum_{ss's'',\alpha\beta\gamma,l',l''}[C_{ss's'',\alpha\beta\gamma}(l,l',l'')u_{s,\alpha}(\mathbf{q},j_1)u_\beta(j_2)u_{s'',\gamma}(\mathbf{q}'',j_3)\\ &\quad+C_{ss's'',\alpha\beta\gamma}(l,l',l'')u_{s,\alpha}(\mathbf{q},j_1)u^{s'}_{\beta,\beta'}(j_2)q'_{\beta'}u_{s'',\gamma}(\mathbf{q}'',j_3)]e^{-i(\mathbf{q}\cdot\mathbf{R}+\mathbf{q}''\cdot\mathbf{R}^{l''})}\\ &\quad\times[1-i\mathbf{q}'\cdot\mathbf{R}^{l'}+\mathcal{O}(-i(\mathbf{q}'\cdot\mathbf{R}')^2)].\end{aligned} \tag{B9}$$

We find that the lowest order term in the right-hand side contains the sum

$$\sum_{l',s'} C_{ss's'',\alpha\beta\gamma}(l,l',l'')u_\beta(j_2)=0, \tag{B10}$$

where we have used the sum rule Eq. (B3). It is easy to see that, in general, the remaining terms vanish linearly in $\mathbf{q}'$. Since in the long-wavelength limit the frequency of an acoustic phonon vanishes like $\omega_A(\mathbf{q}')=c(\hat{\mathbf{q}}')|\mathbf{q}'|$ ($\hat{\mathbf{q}}'$ indicates a unit vector), with the help of Eq. (B4) and Eq. (B5) we obtain, after some straightforward algebra, that

$$2\Gamma_{\mathrm{O}\to A+\mathrm{O}}=a(\hat{\mathbf{q}}')|\mathbf{q}'|, \tag{B11}$$

where a is a constant that can depend of the direction of $\mathbf{q}'$ (we have omitted terms of higher order). In a similar way we can prove that

$$2\Gamma_{\mathrm{O}\to A+A}=|\mathbf{q}'|b(\hat{\mathbf{q}}',\hat{\mathbf{q}}'')|\mathbf{q}''|, \tag{B12}$$

i.e., the decay process involving two acoustic phonons must vanish quadratically in the long-wavelength limit (b is a constant that can depend on the orientation of the two acoustic phonons). It is easy to generalize these formulas to decay processes involving all possible combinations of phonon branches. Our results explain why the decay processes that involve acoustic phonons near the Brillouin zone center give in general small contributions to the Raman linewidths in comparison to the other decay channels.

[1] H. Bilz and W. Kress, *Phonon Dispersion Relation in Insulators* (Springer, Berlin, 1979).

[2] See, for example, N. W. Ashcroft and N. D. Mermin, *Solid State Physics* (Holt-Saunders, Tokyo, 1976).

[3] For a review, see J. A. Kash and J. C. Tsang, in *Light Scattering in Solids VI*, edited by M. Cardona and G. Güntherodt (Springer, Berlin, 1991), p. 423.

[4] J. Menéndez and M. Cardona, Phys. Rev. B **29**, 2051 (1984).

[5] For a review, see M. Cardona *et al.*, J. Phys.: Condens. Matter **5**, A61 (1993).

[6] R. A. Cowley, J. Phys. (France) **26**, 659 (1965).
[7] See, e.g., G. P. Srivastava, *The Physics of Phonons* (Hilger, Bristol, 1990).
[8] S. Baroni, P. Giannozzi, and A. Testa, Phys. Rev. Lett. **58**, 1861 (1987).
[9] P. Giannozzi, S. de Gironcoli, P. Pavone, and S. Baroni, Phys. Rev. B **43**, 7231 (1991).
[10] See, for example, L. I. Schiff, *Quantum Mechanics* (McGraw-Hill, New York, 1968), p. 246.
[11] X. Gonze and J. P. Vigneron, Phys. Rev. B **39**, 13 120 (1989).
[12] A. Debernardi and S. Baroni, Solid State Commun. **91**, 813 (1994).
[13] A. Debernardi, S. Baroni, and E. Molinari, Phys. Rev. Lett. **75**, 1819 (1995).
[14] A. Debernardi, S. Baroni, and E. Molinari, in *Proceedings of the 22nd International Conference on the Physics of Semiconductors*, edited by D. J. Lockwood (World Scientific, Singapore, 1994), p. 373.
[15] A. Debernardi, Ph.D. thesis, Scuola Internazionale Superiore di Studi Avanzati, Trieste, 1995, http://www.sissa.it/cm/-CMsector/PHD.html.
[16] C. Ulrich, E. Anastassakis, K. Syassen, A. Debernardi, and M. Cardona, Phys. Rev. Lett. **78**, 1283 (1997).
[17] As applies to Raman scattering except for very small angle forward scattering. A discussion of the limit of the phonon frequencies for vanishing **q** can be found in R. M. Pick, Adv. Phys. **19**, 269 (1970).
[18] Note that cubic symmetry requires this splitting to disappear at exactly $\mathbf{q}=\mathbf{0}$.
[19] See, for example, A. A. Maradudin, E. W. Montroll, G. H. Weiss, and I. P. Ipatova, *Theory of Lattice Dynamics in the Harmonic Approximation*, edited by H. Ehrenreich, F. Seitz, and D. Turnbull (Academic Press, New York, 1971).
[20] W. Cochran and R. A. Cowley, J. Phys. Chem. Solids **23**, 447 (1962).
[21] R. M. Pick, M. H. Cohen, and R. M. Martin, Phys. Rev. B **1**, 910 (1970).
[22] R. Resta, Phys. Rev. B **27**, 3620 (1983).
[23] D. M. Ceperley and B. J. Alder, Phys. Rev. Lett. **45**, 566 (1980).
[24] J. P. Perdew and A. Zunger, Phys. Rev. B **23**, 5048 (1981).
[25] U. von Barth and R. Car (unpublished).
[26] A. Baldereschi, Phys. Rev. B **7**, 5212 (1973); D. J. Chadi and M. L. Cohen, *ibid.* **8**, 5747 (1973); D. J. Chadi, *ibid.* **16**, 1746 (1977).
[27] H. J. Monkhorst and J. D. Pack, Phys. Rev. B **13**, 5188 (1976).
[28] O. Jepsen and O. K. Andersen, Solid State Commun. **9**, 1763 (1971).
[29] G. Lehman and M. Taut, Phys. Status Solidi B **54**, 469 (1972).
[30] *Numerical Data and Functional Relationship in Science and Technology*, edited by O. Madelung, Landolt-Börastein, New Series, Vol. 17, Part a (Springer, New York, 1982).
[31] G. Lucovsky, R. M. Martin, and E. Burstein, Phys. Rev. B **4**, 1367 (1971).
[32] The effect of isotopic disorder on the TO linewidths of GaAs was recently studied with infrared spectroscopy; R. Henn, Ph.D. thesis, Max-Planck-Institut für Festkörperforschung, Stuttgart, 1997.
[33] B. Kh. Bairamov, Yu. É. Kitaev, V. K. Negoduiko, and Z. M. Khashkhozhev, Fiz. Tverd. Tela (Leningrad) **16**, 2036 (1974) [Sov. Phys. Solid State **16**, 1323 (1975)].
[34] G. Irmer, M. Wenzel, and J. Monecke, Phys. Status Solidi B **195**, 85 (1996).
[35] F. Vallée and F. Bogani, Phys. Rev. B **43**, 12 049 (1991).
[36] E. T. M. Kernohan, R. T. Phillips, B. H. Bairamov, D. A. Ritchie, and M. Y. Simmons, Solid State Commun. **100**, 263 (1996).
[37] F. Vallée, Phys. Rev. B **49**, 2460 (1994).
[38] W. E. Bron, J. Kuhl, and B. K. Rhee, Phys. Rev. B **34**, 6961 (1986).
[39] J. Kuhl and W. E. Bron, Solid State Commun. **49**, 935 (1984).
[40] B. Kh. Bairamov, D. A. Parshin, V. V. Toporov, and Sh. B. Ubaidullaev, Sov. Tech. Phys. Lett. **5**, 486 (1979).
[41] Note that in Bairamov's work the instrumental linewidth was 0.14 cm^{-1}, comparable with the linewidth measured. See Fig. 2 of Ref. 33.
[42] F. Vallée, Solid State Commun. **93**, 741 (1995).
[43] D. von der Linde, J. Kuhl, and H. Klingenberg, Phys. Rev. Lett. **44**, 1505 (1980).
[44] B. A. Weinstein, Solid State Commun. **20**, 999 (1976).
[45] B. A. Weinstein and G. J. Piermarini, Phys. Rev. B **12**, 1172 (1975).
[46] M. T. Yin and M. L. Cohen, Phys. Rev. B **26**, 3259 (1982).
[47] R. Resta, Phys. Rev. B **44**, 11 035 (1991).
[48] The present calculation of $\gamma(\omega)$ has been performed by broadening $\delta(\omega-\omega_j)$ with a Gaussian whose width is 10 cm^{-1}.